Brain Research

Research Report

P50: A candidate ERP biomarker of prodromal Alzheimer's disease

CrossMark

Deborah L. Green[a,*,1], Lisa Payne[b,2], Robi Polikar[c], Paul J. Moberg[d], David A. Wolk[e], John Kounios[a]

[a]Department of Psychology, Drexel University, Stratton Hall, 3141 Chestnut Street, Philadelphia, PA 19104, USA
[b]Volen National Center for Complex Systems, Brandeis University, 145 South Street, Waltham, MA 02453, USA
[c]Department of Electrical and Computer Engineering, Rowan University, 201 Mullica Hill Road, Glassboro, NJ 08028, USA
[d]Department of Neuropsychiatry, University of Pennsylvania, 10th floor, Gates Building, 3401 Spruce Street, Philadelphia, PA 19104, USA
[e]Department of Neurology, University of Pennsylvania, Ralston House, 3615 Chestnut Street, Philadelphia, PA 19104, USA

ABSTRACT

Introduction: Reductions of cerebrospinal fluid (CSF) amyloid-beta (Aβ42) and elevated phosphorylated-tau (p-Tau) reflect in vivo Alzheimer's disease (AD) pathology and show utility in predicting conversion from mild cognitive impairment (MCI) to dementia. We investigated the P50 event-related potential component as a noninvasive biomarker of AD pathology in non-demented elderly.
Methods: 36 MCI patients were stratified into amyloid positive (MCI-AD, $n=17$) and negative (MCI-Other, $n=19$) groups using CSF levels of Aβ42. All amyloid positive patients were also p-Tau positive. P50s were elicited with an auditory oddball paradigm.
Results: MCI-AD patients yielded larger P50s than MCI-Other. The best amyloid-status predictor model showed 94.7% sensitivity, 94.1% specificity and 94.4% total accuracy.
Discussion: P50 predicted amyloid status in MCI patients, thereby showing a relationship with AD pathology versus MCI from another etiology. The P50 may have clinical utility for inexpensive pre-screening and assessment of Alzheimer's pathology.

Published by Elsevier B.V.

1. Introduction

Cerebrospinal fluid (CSF) levels of amyloid-beta (Aβ42) and phosphorylated tau (p-Tau) are thought to reflect in vivo Alzheimer's disease (AD) pathology and have shown promise for identifying patients early in the disease course prior to the onset of dementia. Reductions in CSF Aβ42 correspond with the presence of amyloid plaques in the brain, with CSF levels

approximately 50% lower in AD patients than in controls (Blennow et al., 2015). MCI patients also show AD-like reductions in CSF Aβ42, with baseline levels predicting conversion to AD dementia almost 5 years later (Hertze et al., 2010).

In contrast to CSF biomarkers, measurement of event-related potentials (ERP) is noninvasive, inexpensive, and more widely available. ERPs can reveal abnormalities in brain activity that reflect underlying disease-related changes in the brain. Abnormal ERPs have been documented in AD patients and in patients with mild cognitive impairment (MCI) (Goodin et al., 1978). In particular, recent studies have shown that the P50 differentiates mild AD patients from age-matched controls, and may have utility in predicting MCI conversion to dementia (Golob et al., 2002, 2007).

The P50 is a positive-going wave peaking approximately 50 ms after the onset of an auditory stimulus. It is produced in primary and secondary auditory cortices, though its amplitude is modulated by frontal brain regions and is typically maximal at the vertex electrode (Korzyukov et al., 2007). P50 amplitude is influenced primarily by exogenous factors, such as the physical features of a stimulus, rather than by endogenous cognitive factors, such as expectations and evaluation of the environment (Picton et al., 1974). P50 amplitude also reflects the inhibition of irrelevant or distracting stimuli, a process known as *sensory gating* when taking place at an early sensory stage of processing (Boutros and Belger, 1999).

One standard technique for investigating the filtering out of task-irrelevant information is the *oddball paradigm* in which participants are asked to identify infrequent targets embedded in a series of frequently occurring distractor stimuli (Golob et al., 2007). Successful inhibition of irrelevant information, indicating normal cognitive functioning, is reflected by larger amplitude responses to targets relative to distractors. Individuals with a large P50 response to distractors show impaired inhibition.

Using an oddball paradigm, Golob and Starr (2000) found larger P50 amplitude in response to distractors in mild-AD patients relative to age-matched controls. More recently, the M50, the magnetic counterpart of the P50, was found to be larger in mild-AD patients relative to young and older controls (Cheng et al., 2012). Methodological differences complicate comparison across studies; however, studies that failed to show significantly larger P50 amplitudes in AD patients relative to those from age-matched controls have included a more severe cohort in the mild-to-moderate AD range (e.g., MMSE=13.2±5.4) (Golob et al., 2007) than in the very mild range (e.g, MMSE=23±0.9)(Cheng et al., 2012; Golob and Starr,

2000). In contrast, P50 latency has been comparable between clinical groups and age-matched controls (Cheng et al., 2012; Golob and Starr, 2000; Golob et al., 2007; Irimajiri et al., 2005, 2010) in all but one study that found longer latencies in MCI patients and a correlation between larger amplitude and longer latency P50 response to distractor tones (Golob et al., 2002).

P50 amplitude increases with normal aging (Amenedo and Díaz, 1999; Azumi et al., 1995; Golob et al., 2007), but greater amplitude increase is observed in MCI patients relative to age-matched controls (Golob et al., 2002, 2007; Irimajiri et al., 2005). Amnestic MCI patients with deficits in multiple cognitive domains, who have the highest risk of conversion to AD, show larger P50 amplitudes than single-domain amnestic MCI (Golob et al., 2007). In small samples, MCI to AD converters have also shown baseline P50 amplitudes greater than their stable counterparts (Golob et al., 2002, 2007).

Overall, the literature suggests that P50 amplitude first increases during early stage AD and then decreases back to relatively normal levels with disease progression, possibly because the disease first attacks inhibitory mechanisms that restrain the P50 and only later does it impair the sensory cortical areas primarily responsible for generating the P50, consistent with the progression of underlying AD neuropathology (Arnold et al., 1991; Golubic et al., 2014). While this relationship between P50 and disease severity would be problematic for using P50 in differential diagnosis, when amplitudes may be going up or coming down and indistinguishable from controls, it may have utility as a pre-screening tool during prodromal and asymptomatic stages, when inhibitory mechanisms, but not the neural generators of P50, are compromised.

2. Results

2.1. Demographic and clinical comparisons

The MCI-AD and MCI-Other groups were comparable in age, $t(34)=1.09$, $p=0.49$, and gender, $\chi^2(1, 36)=0.34$, $p=0.56$ (Table 1). The MCI-AD group was more highly educated than the MCI-Other group, $U(36)=246.00$, $p<0.01$. The MCI-AD group was comprised mostly of Non-Latino Caucasians whereas the MCI-Other group was largely split between Non-Latino Caucasians and self-identified, Multiracial Latinos, $\chi^2(3, 36)=10.53$, $p=0.02$.

Clinically, the groups did not differ in symptom severity as measured by the MMSE, $U(36)=143.50$, $p=0.57$, $r=0.09$. The

Table 1 – Demographic and clinical information.		
	MCI-AD	MCI-Other
N	19	17
M/F	5/14	6/11
Age M(SD)	70.95 (6.72)	68.09 (8.93)
Age symptom onset M(SD)	66.58 (6.64)	65.44 (8.18)
Symptom duration Mdn (range) years *	3 (1–13)	2 (1–8)
Education Mdn (range) years *	16 (11–20)	12 (4–18)
MMSE M (SD)	25.89 (2.81)	26.41 (2.83)

* $p<0.05$.

groups did not differ in the age of symptom onset, $t(33)=0.46$, $p=0.65$, but the MCI-AD group had a longer time-lag between symptom onset and EEG data collection (mean=5 years) compared to the MCI-Other group (mean=2 years), $U(35)=235.50$, $p=0.005$, $r=0.48$ (one value missing). There was no difference in the amount of time between EEG and CSF data collection for the MCI-AD (median=36 days) and MCI-Other (median=49 days) groups, $U(36)=138.50$, $p=0.47$.

2.2. P50 amplitude comparison MCI-AD vs. MCI-Other

Compared to the MCI-Other group, the MCI-AD group showed larger P50 amplitude in response to standard (distractor) tones, as hypothesized, as well as larger P50 amplitude in response to target and novel tones. Grand average waveforms were computed for each group separately in response to standard, target, and novel stimuli (Fig. 1). Mean amplitude comparisons are shown in Table 2.

Relevant between-group effects included a significant anterior/posterior × group interaction for the midline ANOVA, $F(1, 34)=6.11$, $p=0.006$. In the overall ANOVA, there were marginally significant anterior/posterior × hemisphere × group, $F(1, 34)=4.06$, $p=0.052$, and hemisphere × stimulus × group, $F(2, 33)=2.73$, $p=0.076$, interactions.

Significant main effects for stimulus condition were found in the overall and midline ANOVAs, $F(2, 33)=10.30$, $p<0.001$ and $F(2, 33)=7.42$, $p=0.002$, respectively. For midline electrodes, there was also a significant anterior/posterior × stimulus interaction, $F(2, 33)=5.25$, $p=0.008$.

Nonparametric follow-up comparisons revealed significantly larger P50 amplitudes for the MCI-AD compared to the MCI-Other group for standard and novel stimuli at all frontal and central but not parietal sites. In response to targets, the MCI-AD group showed larger P50 amplitude at frontal and central electrode locations (with the exception of a nonsignificant difference at F3), as well as larger P50 at posterior sites (P3 and Pz). Of the electrodes not included in the ANOVAs, only in response to novels at Oz did the MCI-Other group show larger P50 than the MCI-AD group. Frequency distribution histograms for P50 amplitude at the vertex are presented in Fig. 2.

2.3. P50 latency comparison MCI-AD vs. MCI-Other

P50 latency varied as function of scalp location, but there were no significant between-group or stimulus effects. A repeated-measures ANOVA using the midline electrodes revealed no significant effects for the group or stimulus condition factors.

2.4. Diagnostic classification of MCI-AD vs. MCI-Other

Logistic regression analysis revealed P50 amplitude was a significant predictor of CSF status using P50 amplitude at the vertex and years of education as predictor variables. A test of the full logit model versus a model with intercept only was statistically significant for standard, $\chi^2(2, 36)=23.59$, $p<.001$; target, $\chi^2(2, 36)=15.31$, $p<.001$; and novel stimuli $\chi^2(2, 36)=14.24$, $p=.001$. Table 3 shows the summary variables of interest for each model. For standard tones, holding education constant, a $1\,\mu V$ increase in amplitude at Cz was associated with a 7-fold increase in the odds of amyloid positivity. P50 amplitude at left-central electrode C3 in response to standards was found to be the best predictor,
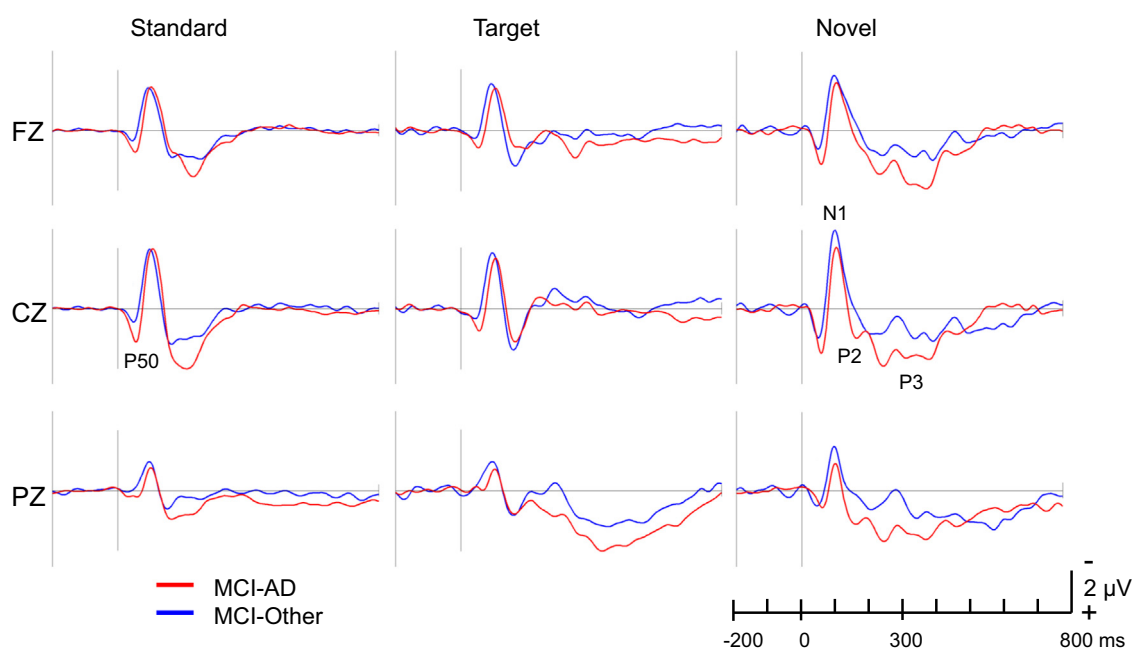

Fig. 1 – ERP Grand average waveforms at frontal (Fz), central (Cz) and parietal (Pz) midline electrodes in response to standard, target, and novel stimuli. Time goes from left to right on the horizontal axis. Negative voltages are plotted up on the vertical axis according to convention. ERPs were computed with a 200 ms baseline prior to stimulus onset (at 0 ms). A 25-Hz lowpass filter was applied prior to individual ERP computation. The P50 component is indicated in the standard ERP at electrode Cz. The N1, P2, and P3 components are indicated in the novel ERP at electrode Cz.

Table 2 – P50 Amplitude (μV) comparisons for the MCI groups.

|		Standard		Target		Novel	
		MCI-AD	MCI-Other	MCI-AD	MCI-Other	MCI-AD	MCI-Other
F3	M	0.65[a]	−0.19[a]	0.46	−0.13	1.25[c]	0.39[c]
	SD	1.11	0.79	1.39	0.69	1.38	1.06
F4	M	0.78[a]	−0.004[a]	0.75[b]	−0.42[b]	1.41[c]	0.38[c]
	SD	0.89	0.86	1.33	0.91	1.03	0.94
Fz	M	0.48[a]	−0.27[a]	0.45[b]	−0.40[b]	0.45[c]	0.20[c]
	SD	0.99	0.89	1.42	0.65	1.42	0.92
C3	M	1.35[a]	0.08[a]	0.87[b]	−0.18[b]	1.92[c]	0.89[c]
	SD	1.16	1.03	1.33	0.82	1.48	1.25
C4	M	1.11[a]	0.09[a]	0.86[b]	−0.19[b]	1.67[c]	0.85[c]
	SD	0.95	1.03	1.26	0.72	1.29	1.19
Cz	**M**	**1.02[a]**	**−0.08[a]**	**0.77[b]**	**−0.31[b]**	**1.50[c]**	**0.60[c]**
	SD	**1.01**	**0.97**	**1.39**	**0.87**	**1.31**	**1.31**
P3	M	0.30	−0.33	−0.04[b]	−0.53[b]	0.67	−0.53
	SD	1.03	0.93	1.13	0.68	0.89	0.68
P4	M	0.12	−0.14	−0.009	−0.33	0.56	0.43
	SD	0.84	0.93	1.09	0.66	0.94	1.15
Pz	M	0.16	−0.38	−0.08[b]	−0.62[b]	0.51	0.26
	SD	0.87	1.01	0.95	0.67	0.98	1.11

Note. Mann-Whitney U-Test computed for between-group comparisons.
[a] $p < 0.05$ for standard stimuli.
[b] $p < 0.05$ for target stimuli.
[c] $p < 0.05$ for novel stimuli.
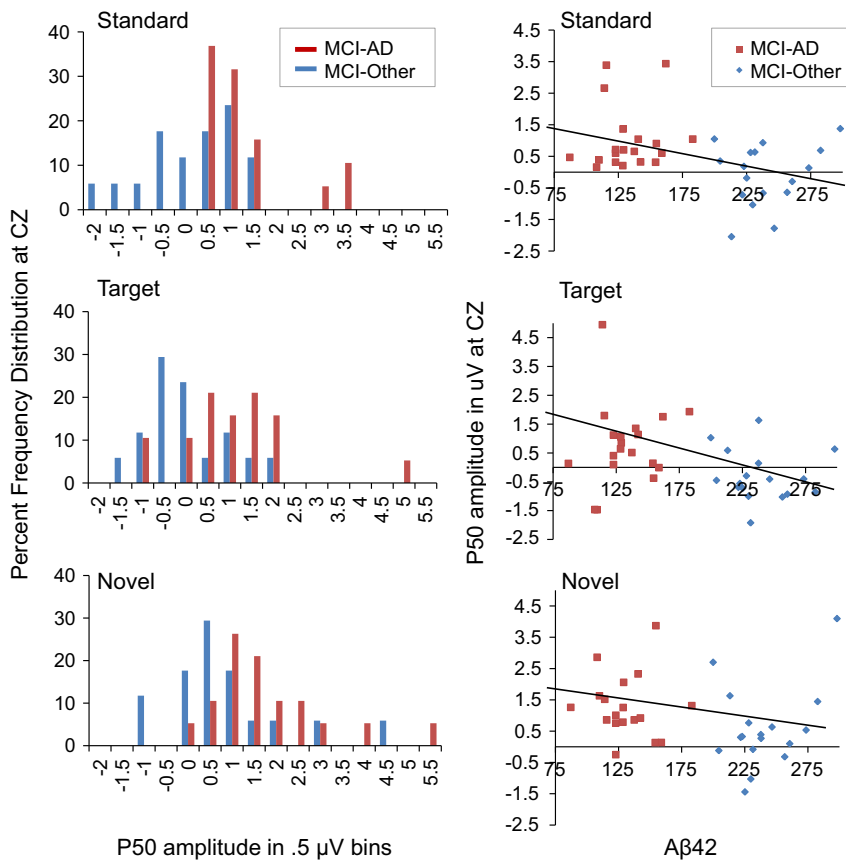
Fig. 2 – Frequency distributions of P50 amplitudes at electrode Cz, showing the percentage of participants with values within each .5 μV bin (left). Regression lines overlay scatterplots of P50 amplitudes at electrode Cz and CSF Aβ42 for all stimuli (right).

Table 3 – Logistic regression predicting CSF Status from P50 amplitude and years education.

	Predictors	B	Wald χ^2	p	Odds ratio
Standard	P50 at C3	2.17	6.424	0.011	8.745
	Education	0.564	6.957	0.008	1.757
Standard	P50 at Cz	1.947	5.890	0.015	7.006
	Education	0.396	6.848	0.009	1.485
Target	P50 at Cz	0.814	3.493	0.062	2.256
	Education	0.286	5.156	0.023	1.331
Novel	P50 at Cz	0.659	2.935	0.087	1.933
	Education	0.325	6.365	0.012	1.384

Classification accuracy of logistic regression models predicting CSF status.

	SEN	SPEC	PPV	NPV	Total accuracy	Nagelkerke's R^2
Standard C3	94.7	94.1	94.7	94.1	94.4	0.72
Standard Cz	84.2	88.2	88.9	83.3	86.1	0.64
Target Cz	78.9	76.5	78.9	76.5	77.8	0.46
Novel Cz	78.9	82.4	83.3	77.8	80.6	0.44

Note. SEN=sensitivity; SPEC=specificity; PPV=positive predictive value; NPV=negative predictive value.

with 94.7% sensitivity, 94.1% specificity, and total model accuracy of 94.4%. Scatterplots of P50 amplitude at C3 and Aβ42 are presented in Fig. 3.

Partial correlation controlling for education revealed a significant negative relationship between Aβ42 and standard P50 amplitude at Cz, $r=-0.42$, $p=0.013$, with marginally significant findings for targets at Cz, $r=-0.32$, $p=0.060$. There was a not a significant linear relationship between Aβ42 and P50 amplitude in response to novels, $r=-0.18$, $p=0.31$.

2.5. Analysis of N1, P2, P3 ERP components

Repeated measures ANOVAs using midline electrodes (Fz, Cz, and Pz) revealed no significant group effects on amplitude or latency of the N1, P2, or P3 ERP components.

3. Discussion

This study investigated P50 as a potential biomarker of early AD pathology and found that P50 amplitude predicted CSF status in MCI patients. Amyloid- and p-Tau positive MCI patients showed larger P50 amplitudes for all stimulus conditions relative to the amyloid-negative group. These findings are consistent with preliminary evidence that MCI patients who convert to AD show larger P50 amplitudes at baseline relative to non-converters (Golob et al., 2002, 2007). Larger P50 amplitudes to standard stimuli have been interpreted as a deficit in sensory gating (Cheng et al., 2012; Golob et al., 2007). However, the present findings of larger P50s to target and novel stimuli as well suggest a more general deterioration of inhibitory regulation of auditory cortex.

Findings from EEG, MEG, and fMRI cross-modal sensory gating studies, frontal lesion studies, and from auditory brain stem responses implicate prefrontal cortex (PFC) in the top-down inhibition of the auditory cortical response (Golubic et al., 2014; Irimajiri et al., 2005; Knight et al., 1989; Mayer
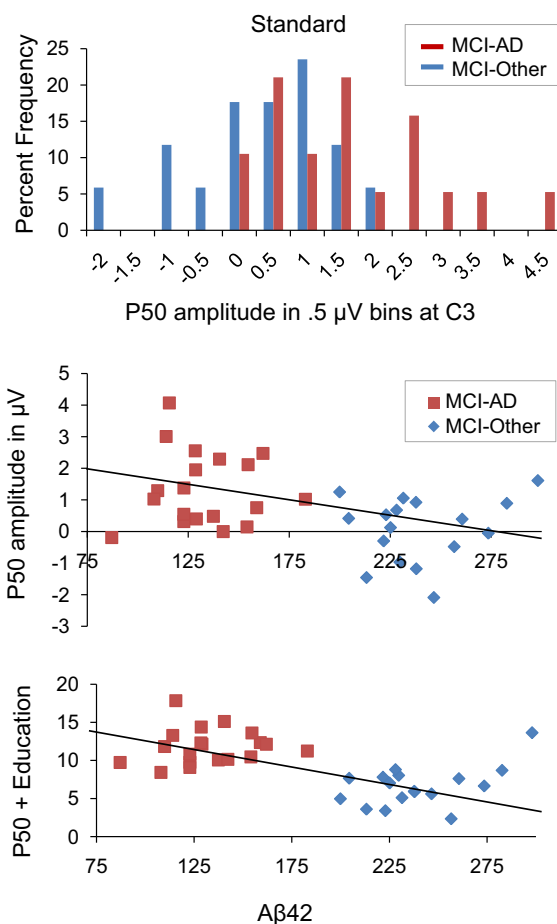
Fig. 3 – Frequency distribution of P50 amplitude at electrode C3, showing the percentage of participants with values within each .5 μV bin (top). Partial correlation controlling for education revealed a significant negative relationship between Aβ42 and standard P50 amplitude at C3, $r=-0.49$, $p=0.003$ (middle). P50 and years education as predictors of Aβ42 (bottom).

et al., 2009; Oranje et al., 2006; Tregellas et al., 2007; Weiland et al., 2008). Evidence from animal models and human fMRI studies suggests that the PFC may influence the activity of auditory cortex directly or via projections through the thalamus (Mayer et al., 2009; Yingling and Skinner, 1976). Recent M50 localization findings support this hypothesis; healthy elderly showed both prefrontal and superior temporal sources modulating M50 amplitude whereas cognitively impaired elderly showed a temporal but not prefrontal source, which was associated with larger amplitudes in the absence of PFC contributions (Golubic et al., 2014). Unrestrained P50 amplitude may therefore represent a functional disconnection of the prefrontal cortex in modulating the auditory cortical response. This view is supported by findings of general cortical disconnection in AD, including lower frontal-parietal correlations of glucose metabolism and less frontal-posterior coherence of electrical activity in the brain (Leuchter et al., 1992; Rapoport et al., 1986).

In sum, the present results suggest that P50 may prove to be a useful biomarker for early, even pre-symptomatic, AD. The fact that it can be recorded noninvasively and inexpensively may make it a practical diagnostic or screening tool that could help clinicians to optimize therapeutic interventions or even to help in the selection of additional costly or invasive tests (e.g., amyloid PET). Future longitudinal studies can evaluate the utility of P50 to predict cognitive decline and conversion to dementia by tracking P50 changes in cognitively intact, amyloid positive and negative individuals, including those with and without evidence of p-Tau pathology.

4. Experimental procedure

4.1. Participants

Participants were recruited by researchers at the University of Pennsylvania for several longitudinal studies dedicated to the evaluation and management of neurodegenerative diseases. All participants signed consent forms in compliance with the University of Pennsylvania's IRB-approved protocol. Thirty-six MCI patients (25 women) were included in the present study. Participants were evaluated at the University of Pennsylvania by clinical history taking, family interviews, neurological evaluation, and neuropsychological evaluation. All but one participant was community dwelling; one MCI patient lived in an assisted living facility. MCI patients had no history of neurological disease but reported evidence of new-onset cognitive decline that was corroborated by a collateral informant and objectively demonstrated on neuropsychological testing and clinical exam. The MCI group, however, did not meet diagnostic criteria for dementia at the time of the evaluation. MCI patients were divided into amyloid positive (MCI-AD, $n=19$) and amyloid negative (MCI-Other, $n=17$) groups. All MCI-AD patients were Aβ42 and p-Tau positive based on published, validated diagnostic cutoff values, i.e., Aβ42 below 192 pg/mL, p-Tau above 23 pg/mL (De Meyer et al., 2010; Shaw et al., 2009). Six of the 17 MCI-Other patients were positive for only p-Tau.

4.2. Auditory stimuli and experimental procedures

Eight-hundred and sixty-four computer-generated stimuli were presented with an interstimulus interval that varied randomly from 1.0 to 1.3 s. High-pitched, 2000-Hz target tones (100-ms duration, $n=172$) were randomly interspersed among low-pitched, 1000-Hz standard tones (100-ms duration, $n=560$) (Yamaguchi et al., 2000). One-hundred and thirty-two unique, unrepeated, novel environmental sounds (200-ms duration) were also interspersed, following a common version of the oddball paradigm previously used for AD research (Yamaguchi et al., 2000). Auditory stimuli were presented via external speakers flanking the computer monitor. Volume levels were individually adjusted to a comfortable, audible level for each participant. Hearing aids were permitted. Stimulus presentation took place across six 3-minute experimental blocks. Participants were instructed to focus their eyes on a fixation cross on the computer screen in front of them and to press a button to identify target tones while ignoring all other stimuli.

4.3. Recordings and data processing

Gold scalp electrodes were used to record EEGs from 16 channels placed according to the International 10–20 System (Homan et al., 1987). A g.Power–g.USBamp biosignal amplifier continuously amplified and digitized the EEG signal (sampling rate: 256 Hz, bandpass:0.02–100 Hz, 4 independent grounds; g-tec Medical Engineering). The BCI2000 platform was used for stimulus presentation and EEG data acquisition (Schalk et al., 2004). Due to hardware malfunction, the behavioral data are unreliable and are not reported here.

Independent components analysis (ICA)(Delorme and Makeig, 2004) followed by manual inspection were used to identify and eliminate ocular and other artifacts. A 25-Hz low-pass filter was applied prior to computation of ERP averages for each stimulus condition. P50 amplitude was computed by averaging the amplitude measurements across the 42–78 ms post-stimulus time window.

4.4. CSF collection and analysis

CSF samples were obtained by standard clinical lumbar puncture following the Alzheimer's Disease Neuroimaging Initiative protocol (Shaw et al., 2009). Aβ42 was measured using the multiplex xMAP Luminex platform (Luminex Corp, Austin, TX) with Innogenetics (INNO-VIA AlzBio3, Ghent, Belgium) immunoassay kit-based reagents.

4.5. Evaluation of disease severity

All participants were evaluated with the Mini-Mental State Exam (MMSE), a widely used, brief screening measure of global cognitive functioning (Folstein et al., 1975).

4.6. Data analysis overview

Between-group comparisons of demographic and clinical variables were computed using independent-samples t-tests,

Mann-Whitney U-tests, and Pearson chi-square tests where appropriate.

Two repeated measures ANOVAs were performed to investigate the relationships among P50 amplitude, stimulus type, electrode scalp location, and CSF status. The first overall ANOVA included the between-group factor of CSF status (MCI-AD, MCI-Other; 2 levels) and the within-group factors of anterior/posterior electrode location (2 levels), hemisphere (2 levels), and stimulus condition (target, standard, novel; 3 levels). The electrodes included in this analysis were F3/F4 and C3/C4, frontal and central areas where P50 amplitude is largest across the scalp. A second repeated measures *midline* ANOVA was used to examine the midline electrodes Fz, Cz, and Pz, including the between-group factor of CSF status (2 levels) and the within-group factors of anterior/posterior location (3 levels) × stimulus (3 levels). Nonparametric follow-up comparisons were computed to explore the between-group differences at each electrode. The Huynh-Feldt correction was used for violations of sphericity and adjusted *p*-values were reported where appropriate. For all analyses, two-tailed p values < 0.05 were considered statistically significant.

Binary logistic regression was conducted to predict the probability of amyloid positivity using P50 amplitude and years of education as predictor variables. Age and gender were explored for inclusion but were not significant predictors of CSF status. Secondary analyses explored all combinations of electrode locations and stimulus conditions to identify the best predictor of CSF status.

Acknowledgments

R E F E R E N C E S

Amenedo, E., Díaz, F., 1999. Ageing-related changes in the processing of attended and unattended standard stimuli. Neuroreport 10, 2383.

Arnold, S.E., Hyman, B.T., Flory, J., Damasio, A.R., Van Hoesen, G. W., 1991. The topographical and neuroanatomical distribution of neurofibrillary tangles and neuritic plaques in the cerebral cortex of patients with Alzheimer's disease. Cereb. Cortex 1, 103–116.

Azumi, T., Nakashima, K., Takahashi, K., 1995. Aging effects on auditory middle latency responses. Electromyogr. Clin. Neurophysiol. 35, 397.

Blennow, K., Dubois, B., Fagan, A.M., Lewczuk, P., de Leon, M.J., Hampel, H., 2015. Clinical utility of cerebrospinal fluid biomarkers in the diagnosis of early Alzheimer's disease. Alzheimer's & Dement. 11, 58–69.

Boutros, N.N., Belger, A., 1999. Midlatency evoked potentials attenuation and augmentation reflect different aspects of sensory gating. Biol. Psychiatry 45, 917–922.

Cheng, C.-H., Wang, P.-N., Hsu, W.-Y., Lin, Y.-Y., 2012. Inadequate inhibition of redundant auditory inputs in Alzheimer's disease: an MEG study. Biol. Psychol. 89, 365–373.

De Meyer, G., Shapiro, F., Vanderstichele, H., Vanmechelen, E., Engelborghs, S., De Deyn, P.P., Coart, E., Hansson, O., Minthon, L., Zetterberg, H., 2010. Diagnosis-independent Alzheimer disease biomarker signature in cognitively normal elderly people. Arch. Neurol. 67, 949.

Delorme, A., Makeig, S., 2004. EEGLAB: an open source toolbox for analysis of single-trial EEG dynamics including independent component analysis. J. Neurosci. Methods 134, 9–21.

Folstein, M.F., Folstein, S.E., McHugh, P.R., 1975. Mini-mental state. A practical method for grading the cognitive state of patients for the clinician. J. Psychiatr. Res. 12, 189–198.

Golob, E.J., Starr, A., 2000. Effects of stimulus sequence on event-related potentials and reaction time during target detection in Alzheimer's disease. Clin. Neurophysiol. 111, 1438–1449.

Golob, E.J., Johnson, J.K., Starr, A., 2002. Auditory event-related potentials during target detection are abnormal in mild cognitive impairment. Clin. Neurophysiol. 113, 151–161.

Golob, E.J., Irimajiri, R., Starr, A., 2007. Auditory cortical activity in amnestic mild cognitive impairment: relationship to subtype and conversion to dementia. Brain 130, 740–752.

Golubic, S.J., Aine, C.J., Stephen, J.M., Adair, J.C., Knoefel, J.E., Supek, S., 2014. Modulatory role of the prefrontal generator within the auditory M50 network. NeuroImage 92, 120–131.

Goodin, D.S., Squires, K.C., Starr, A., 1978. Long latency event-related components of the auditory evoked potential in dementia. Brain: J. Neurol. 101, 635.

Hertze, J., Minthon, L., Zetterberg, H., Vanmechelen, E., Blennow, K., Hansson, O., 2010. Evaluation of CSF biomarkers as predictors of Alzheimer's disease: a clinical follow-up study of 4.7 years. J. Alzheimer's Dis. 21, 1119–1128.

Homan, R.W., Herman, J., Purdy, P., 1987. Cerebral location of international 10–20 system electrode placement. Electroencephalogr. Clin. Neurophysiol. 66, 376–382.

Irimajiri, R., Golob, E., Starr, A., 2005. Auditory brain-stem, middle-and long-latency evoked potentials in mild cognitive impairment. Clin. Neurophysiol. 116, 1918–1929.

Irimajiri, R., Golob, E.J., Starr, A., 2010. ApoE genotype and abnormal auditory cortical potentials in healthy older females. Neurobiol. Aging 31, 1799–1804.

Knight, R.T., Scabini, D., Woods, D.L., 1989. Prefrontal cortex gating of auditory transmission in humans. Brain. Res. 504, 338–342.

Korzyukov, O., Pflieger, M.E., Wagner, M., Bowyer, S.M., Rosburg, T., Sundaresan, K., Elger, C.E., Boutros, N.N., 2007. Generators of the intracranial P50 response in auditory sensory gating. Neuroimage 35, 814–826.

Leuchter, A.F., Newton, T.F., Cook, I.A.N.A., Walter, D.O., Rosenberg-Thompson, S., Lachenbruch, P.A., 1992. Changes in brain functional connectivity in Alzheimer-type and multi-infarct dementia. Brain 115, 1543–1561.

Mayer, A., Hanlon, F., Franco, A., Teshiba, T., Thoma, R., Clark, V., Canive, J., 2009. The neural networks underlying auditory sensory gating. Neuroimage 44, 182–189.

Oranje, B., Geyer, M.A., Bocker, K.B.E., Leon Kenemans, J., Verbaten, M.N., 2006. Prepulse inhibition and P50 suppression: commonalities and dissociations. Psychiatry. Res. 143, 147–158.

Picton, T., Hillyard, S., Krausz, H., Galambos, R., 1974. Human auditory evoked potentials: I. Evaluation of components. Electroencephalogr. Clin. Neurophysiol. Electroencephalogr. Clin. Neurophysiol..

Rapoport, S., Horwitz, B., Haxby, J., Grady, C., 1986. Alzheimer's disease: metabolic uncoupling of associative brain regions. Can. J. Neurol. Sci. (Le Journal Canadien des Sciences Neurologiques) 13, 540.

Schalk, G., McFarland, D.J., Hinterberger, T., Birbaumer, N., Wolpaw, J.R., 2004. BCI2000: a general-purpose brain-computer interface (BCI) system. Biomed. Eng. IEEE Trans. 51, 1034–1043.

Shaw, L.M., Vanderstichele, H., Knapik-Czajka, M., Clark, C.M., Aisen, P.S., Petersen, R.C., Blennow, K., Soares, H., Simon, A., Lewczuk, P., 2009. Cerebrospinal fluid biomarker signature in Alzheimer's disease neuroimaging initiative subjects. Ann. Neurol. 65, 403–413.

Tregellas, J.R., Davalos, D.B., Rojas, D.C., Waldo, M.C., Gibson, L., Wylie, K., Du, Y.P., Freedman, R., 2007. Increased hemodynamic response in the hippocampus, thalamus and prefrontal cortex during abnormal sensory gating in schizophrenia. Schizophr. Res. 92, 262–272.

Weiland, B.J., Boutros, N.N., Moran, J.M., Tepley, N., Bowyer, S.M., 2008. Evidence for a frontal cortex role in both auditory and somatosensory habituation: a MEG study. Neuroimage 42, 827–835.

Yamaguchi, S., Tsuchiya, H., Yamagata, S., Toyoda, G., Kobayashi, S., 2000. Event-related brain potentials in response to novel sounds in dementia. Clinical Neurophysiol. 111, 195–203.

Yingling, C.D., Skinner, J.E., 1976. Selective regulation of thalamic sensory relay nuclei by nucleus reticularis thalami. Electroencephalogr. Clin. Neurophysiol. 41, 476.